Modelling of Photovoltaic Plants with Communication Delays based on Field Measurements

1st Luna Moreno-Díaz
Ingelectus SL
Seville, Spain
lmoreno@ingelectus.com

2nd Juan Manuel Mauricio
Department of Electrical Engineering
Universidad de Sevilla
Seville, Spain
jmauricio@us.es

2025 IEEE Kiel PowerTech | 979-8-3315-4397-6/25/$31.00 ©2025 IEEE | DOI: 10.1109/PowerTech59965.2025.11180733

***Abstract*—This paper describes a general methodology for modelling renewable energy plants, in both discrete and continuous time domains, based on field measurements, for control design purposes. The plant model is obtained by applying standard identification techniques to the measured input-output data. It aims to accurately capture the delays and dynamics of the plant in response to sinusoidal power set-points within the frequency range relevant to small-signal electromechanical oscillations (0.1–1.5 Hz). This paper focuses on the communication delays between the central controller and the generation units, as well as the computation time of the devices involved in the centralised plant control. The proposed methodology is applied to an operational medium-scale photovoltaic plant connected to the distribution system of Spain. The identified models are validated against the real system using time-domain simulations and Bode plots, showing an adequate performance in the frequencies of interest.**

***Index Terms*—Photovoltaic plant, communication delays, field tests, identification, centralised control.**

I. Introduction

A. Motivation

The increasing integration of renewable energy plants into the electrical system poses significant technical challenges, with system stability and the loss of inertia being among the most critical issues today [1]. These challenges are of particular concern for Transmission System Operators (TSO), especially those managing weaker grids such as insular or peninsular systems with limited interconnections. In the European framework, the Grid Connection Code (GCC) introduced in 2016 additional grid support services beyond the standard requirements, such as Power Oscillation Damping (POD) and Synthetic Inertia (SI) control [2]. Although these requirements are not yet mandatory in most countries, they have been extensively studied by TSOs in regions with a high penetration of renewable generation, such as Spain [3] [4].

To enable the provision of these advanced grid services from medium and large scale renewable plants centrally controlled at the point of interconnection (POI), accurate modelling of plant dynamics, communication and computation delays is crucial. These factors have a significant impact on the performance and effectiveness of POD and SI controls. Communication delays, in particular, are stochastic in nature and introduce complexity into the system response [5]. Existing analytical models in the literature often simplify these dynamics or consider them in insufficient detail, limiting their applicability to the design, implementation and validation of advanced control strategies. As an alternative, analytical models derived from real system measurements offer a promising approach, providing a detailed representation of the system behaviour for these purposes.

This research is funded by the European Union under the Horizon European project COCOON (GA 101120221) and by MCIN/AEI/10.13039/501100011033/ and FEDER Una manera de hacer Europa under project PID2021-127835OB-I0.

B. Literature review

Renewable power plants are typically modelled for electromechanical grid studies using analytical dynamic models of generators and control systems. A standard approach preferred by some TSOs involves generic positive-sequence dynamic models, such as those developed for the Western Electricity Coordinating Council (WECC) [6], which are widely used in academia and industry. These models allow plant response delays to be represented by a first-order filter with a lag time constant [7]. Alternatively, more accurate user-defined models from manufacturers are used in countries such as Spain [3] and Germany [8], where certified models of individual equipment are required. However, there is no defined method for representing the plant response delay when creating the complete plant model. Current practice approximates these delay by summing the theoretical communication and computation response times of each individual component and using this aggregate value as the time constant in a delay model, such a Padé approximation.

A more precise method for modelling renewable power plants for grid stability studies involves a co-simulation framework that integrates the electrical power system with the communication network. A recent study in [9] incorporates realistic communication delays and reviews existing power and communication co-simulators. Validated on the Irish transmission system, it shows improved accuracy in modeling wide-area control delays compared to mathematical models. The

study highlights a well-known gap in the current modelling of time delays, noting that available references are limited due to theoretical proposals, optimistic assumptions and lack of measurements. While this approach has been widely used for modelling transmission, distribution networks and smart grids [10] [11], it could also be extended to the modelling of renewable energy plants.

Other studies have advanced the field by utilising laboratory environments to measure the response delays of renewable power plants, enabling the development of accurate analytical models for these delays. A recent study focusing on the design of a central POD control for PV plants with communication delays is discussed in [12]. This research presents laboratory measurements of the communication infrastructure and simplifies the observed time-varying delays within the frequency range of interest as a constant average delay. The delay is subsequently modelled using a fourth-order Padé approximation for the design procedure. A similar approach is presented in [13], which addresses the integration of Virtual Synchronous Generator (VSG) technology in PV plants, with a particular focus on modelling communication delays based on experimental measurements.

C. Contributions

This study represents a significant advancement in the field in comparison to previous research, as it employs measurements from a real-world renewable energy plant to develop a precise model of its delays and dynamics. The main contributions of this paper are outlined below:

- To conduct a series of simple and concise field tests on an operational PV plant to accurately capture the delays and dynamic response of the system, which will then be used to develop a model.
- To provide empirical measurements that can be used to validate the mathematical models commonly used in both academia and industry. This addresses the well-acknowledged lack of time response measurements of real-world power systems, a recurring claim in previous research.
- To obtain and validate a continuous and discrete simplified model of a standard PV plant, which can then be used for control design purposes, particularly in applications that require compensation for plant delay response.
- To propose a general methodology for modelling renewable plants. Unlike methods that require detailed representations of both electrical and communication systems, the proposed approach only requires structured field tests and system identification procedures. As a result, it can be applied to any plant, regardless of its size or system configuration.

D. Paper organization

The structure of the paper is as follows: Section II introduces the plant infrastructure and field measurements. Section III explains the procedure for developing an accurate Single-Input Multiple-Output (SIMO) model and its validation. Section IV outlines how this approach can be simplified to create a Single-Input Single-Output (SISO) model, which is used to derive and validate a continuous transfer function for control design. Finally, Section V presents the key findings and future research of this study.

II. Plant Description

The system under study is a conventional medium-scale PV plant, equipped with a standard electrical and communication infrastructure. A comprehensive description of the system is initially provided to offer complete information about the case study. Following this, the field tests conducted to record the plant response are presented in detail.

A. Electrical System

The photovoltaic (PV) power plant under study has a nominal active power of 31.5 MW at the POI, which feeds power into the Medium Voltage (MV) distribution system at 30 kV. This power plant is of the string PV inverter type and is located in Spain. Based on the significance established in the Spanish regulation [2] [14], this is a type C Power Park Module. The electrical layout of the plant is shown in Figure 1-(a). The MV collector system consists of two main feeders that evacuate power from four Secondary Substations (SS) to the POI. Each SS steps up the voltage from 0.80 kV (LV inverter level) to 30 kV (MV distribution level) and has a rated power of 9 MVA. The plant includes 117 PV inverters, each with a nominal AC voltage of 800 V and a nominal power of 300 kVA at 40ºC.

B. Communication System

The communication system responsible for monitoring and controlling the PV plant is shown in Figure 1-(b). This architecture allows the Power Plant Controller (PPC) to receive measurements from the Power Analyser (PA) and send set-points to each PV inverter, ensuring compliance with the applicable requirements of the Spanish Grid Code at the POI [15]. The power analyser collects measurements at the POI and sends them via Modbus TCP/IP over Ethernet to the plant switch. The PPC is connected to the fiber optic network via the plant switch using an Ethernet cable. Communication with the inverters is managed by loggers installed at each SS, which also handle the conversion from fiber optic to Power Line Communication (PLC).

C. Field Measurements

Several field tests were conducted on the PV plant to capture its dynamic response to sinusoidal power references within the frequency range of 0.1 to 1.5 Hz, relevant for small disturbance analysis [3]. These tests allow to observe the dynamic behaviour and damping level of the plant at different frequencies, providing a basis for the design of centralised controllers to improve stability and performance, such as POD and SI control.

A summary of the key test information is provided below:

- Set-point configuration: The power reference signals are sent from the PPC in open loop control mode. This

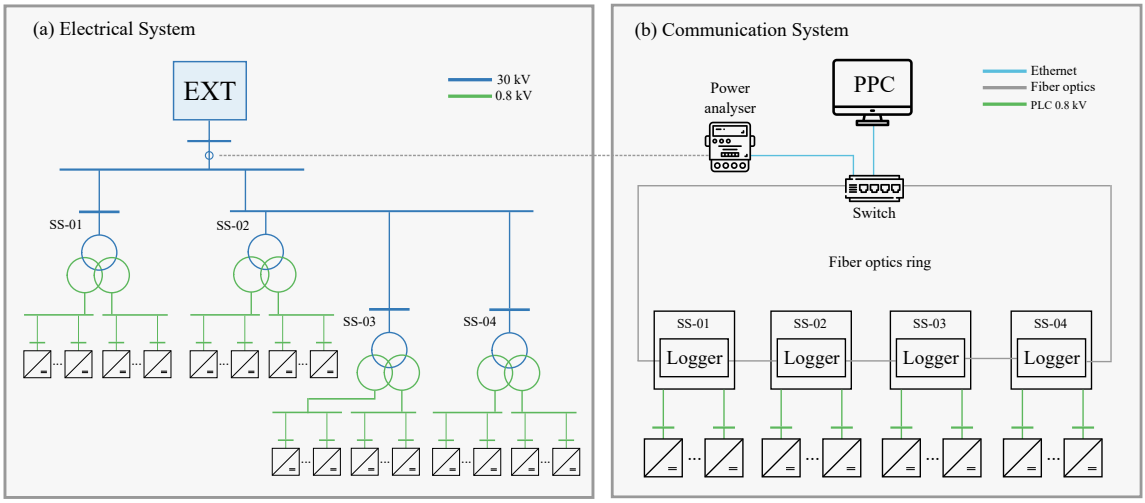

Fig. 1. PV plant electrical (a) and communication (b) single-line diagram

approach allows the dynamic response of the inverters to be measured without adding the effect of the central controller. The minimum configurable sampling time for sending new set-points to the inverters is 250 ms. Several field tests were carried out configuring lower values such as 50, 100 and 150 ms. However, these tests resulted in an inadequate system response.

- Response delays: the delays recorded take place from the time the PPC sends a set-point to the time the power analyser detects the first change in power at the POI. The sequence of communication and computation delays involved in this process is illustrated in Figure 2. In particular, the most significant and uncertain delays occurs between the receipt of the set-point by the logger and the initiation of the response by the inverters. Providing measurements of these delays is a key contribution of this study.
- Data collection: The main data recorded during the tests are the active and reactive power set-points (inputs) and the active and reactive power measured at the POI (outputs). These data are sampled at a rate of 50 ms.
- Field test scenarios: Three field tests were conducted to evaluate scenarios relevant to the design of advanced grid support services, such as a POD central control where three control modes could be activated: POD-P, POD-Q and POD-PQ.
  - P-SIMO data set: variation of the active power reference while the reactive power reference remains constant.
  - Q-SIMO data set: variation of the reactive power reference while the active power reference remains constant.
  - MIMO data set: Simultaneous variation of active and reactive power reference.
- Plant operational status: At the beginning of each test, the plant conditions at the POI were as follows: $P_{POI} = 10.0\,\text{MW} = 0.3175\,\text{pu} \times P_{nom}$, $Q_{POI} = 0.0\,\text{Mvar}$ (power factor = 1).
- Waveform configuration: The power references are varied from their initial value to sinusoidal waveforms with frequencies ranging from 0.1 Hz to 1.4 Hz in increments of 0.1 Hz and an amplitude of $\pm 10\% P_{nom} = \pm 3.15$ MW/Mvar. Each waveform is maintained for a duration sufficient to capture the plant dynamic response at each frequency: 60 seconds for frequencies from 0.1 to 0.5 Hz and 30 seconds for frequencies from 0.6 Hz to 1.4 Hz. The total length of each test is 14 minutes. The waveform described is presented in Fig. 3. A detailed description of this graph is included in section III-B.

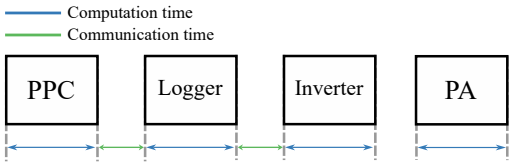

Fig. 2. Field tests response delays

III. SIMO Identification

The identified model is calculated using the time-domain input-output data described in section II-C. This section will focus on the P-SIMO data set in order to not extent the content. The identification is conducted using the Numerical algorithms for Subspace State-Space System (N4SID) method [16]. This method is executed in python with the System Identification Package SIPPY [17]. As a result of this procedure, a discrete identified time-domain model is obtained.

The identification procedure is carried in 2 stages as described in the sections below.

A. System Identification

The first stage is to identify a model using a set of the input-output data. This calculation is depicted in (1):

$$\mathbf{s}ys\_id = system\_identification(z, u, method, SS\_fixed\_order, tsample) \quad (1)$$

$$z = \begin{bmatrix} P_{POI}^{meas} \\ Q_{POI}^{meas} \end{bmatrix} \quad u = \begin{bmatrix} P_{POI}^{ref} \end{bmatrix} \quad (2)$$

Where:

- u, z: the detail of the input vector u and the output matrix z is shown in (2). A subset of the available complete data (0.1 - 1.4 Hz) has to be selected to calculate an identified model of the system. Several data subsets have been tested: 0.1 - 0.4 Hz, 0.1 - 0.5 Hz, 0.1 - 1.0 Hz, among others. Finally, the selected subset is 0.1 - 1.0 Hz.
- $method$: the selected identification method is N4SID. Alternative subspace-based methods, such as the Multiple Output Error State Production (MOESP) and the Canonical Variate Analysis (CVA), have also been tested, not resulting in better results than N4SID.
- SS_fixed_order: another input of this procedure is the order of the identified model. In this case, a 15th-order model is selected to obtain an accurate identified model of the system.
- $tsample$: it is used to build the discrete-time linear model. Given that the input-output data is updated each 50 ms, this value is selected as the sampling time.

B. Validation

The second stage of the process is to validate the identified model in the complete time-domain range by comparing the real and the identified outputs. The validation of the active power at the POI is presented in Fig. 3. The variables represented are as follows: the continuous active power reference (in orange), the discrete active power reference (in red), the active power measured at the POI (in blue) and the identified active power at the POI (in green). The graph is organized in four lines: the first and third line present the complete time-domain data set, while the second and fourth line include a zoom of each frequency from 0.1 to 1.4 Hz.

In general, the active power response of the plant degrades significantly at high frequencies, as the discrete reference sampling time of 250 ms is not sufficient to adequately observe the continuous reference at frequencies of 1.0 Hz and above. In contrast, the response at low frequencies, specifically between 0.1 and 0.3 Hz—those of greatest concern to the Spanish TSO in terms of inter-area oscillations [18]—exhibits satisfactory amplitude and phase behaviour. It can be observed that the amplitude of the response undergoes a gradual attenuation as the frequency increases, with this effect being more pronounced within the range of 1.0 to 1.2 Hz. In terms of phase, frequencies ranging from 0.1 to 0.7 Hz offer a clear depiction of the evolving angle difference between the input and the output, which increases progressively with frequency.

The aforementioned observations apply to the reactive power response depicted in Fig. 4. As a result of the active power reference, the reactive power varies as a waveform with a maximum amplitude of ± 0.3 Mvar, which is equivalent to 10% of the active power reference amplitude. This coupling arises from the change in active power consumption within the plant, which in turn impacts reactive power consumption. Since the plant operates in open-loop control mode, the reactive power measured at the POI it is not adjusted by the PPC to maintain the unit power factor reference.

With regard to the validation of the system identification, the identified output closely aligns with the real output within the low-frequency range of 0.1 to 0.5 Hz, thereby demonstrating high precision in both active and reactive power. However, as the frequency increases, discrepancies in both magnitude and phase arise between the identified output and the real one; nevertheless, the identification still exhibits a satisfactory performance.

IV. SISO Identification

The model presented in section III reveals a small coupling between the active power reference and the reactive power measured at the POI, leading to the use of a SIMO model for a comprehensive representation of the system. However, for control design purposes, the original approach can be simplified by neglecting the coupling between these variables, since the resulting impact on the reactive power remains below 1% of the nominal active power of the plant. Additionally, the reactive power response is further attenuated at higher frequencies, particularly beyond 0.7 Hz. This simplification justifies the use of a SISO model, enabling direct application of the control to a single transfer function of the system.

The identification carried out in this case follows the same approach as the one presented in section III with the appropriate adaptations for a SISO model. With the aim of providing the reader a useful representation of this system for simulation purposes, the identified system will be presented in the state space and Transfer Function (TF) form.

A. System Identification

The identified model is obtained using the calculation proposed in (1) and configuring the following parameters:

$$z = \begin{bmatrix} P_{POI}^{meas} \end{bmatrix} \quad u = \begin{bmatrix} P_{POI}^{ref} \end{bmatrix} \quad (3)$$

- u, z: the input and output data of this case are shown in (3). The same data subset, ranging from 0.1 to 1.0 Hz, has been selected.
- $method$: the selected identification method is N4SID.
- SS_fixed_order: a 2nd-order model is selected to obtain a compact and easy to handle TF of the system.
- $tsample$: the sampling time selected is 50 ms.

The discrete state space form of the identified system is presented as follows:

$$\Delta\dot{\mathbf{x}} = \mathbf{A}\Delta\mathbf{x} + \mathbf{B}\Delta\mathbf{u}, \quad (4)$$

$$\Delta\mathbf{z} = \mathbf{C}\Delta\mathbf{x} + \mathbf{D}\Delta\mathbf{u} \quad (5)$$

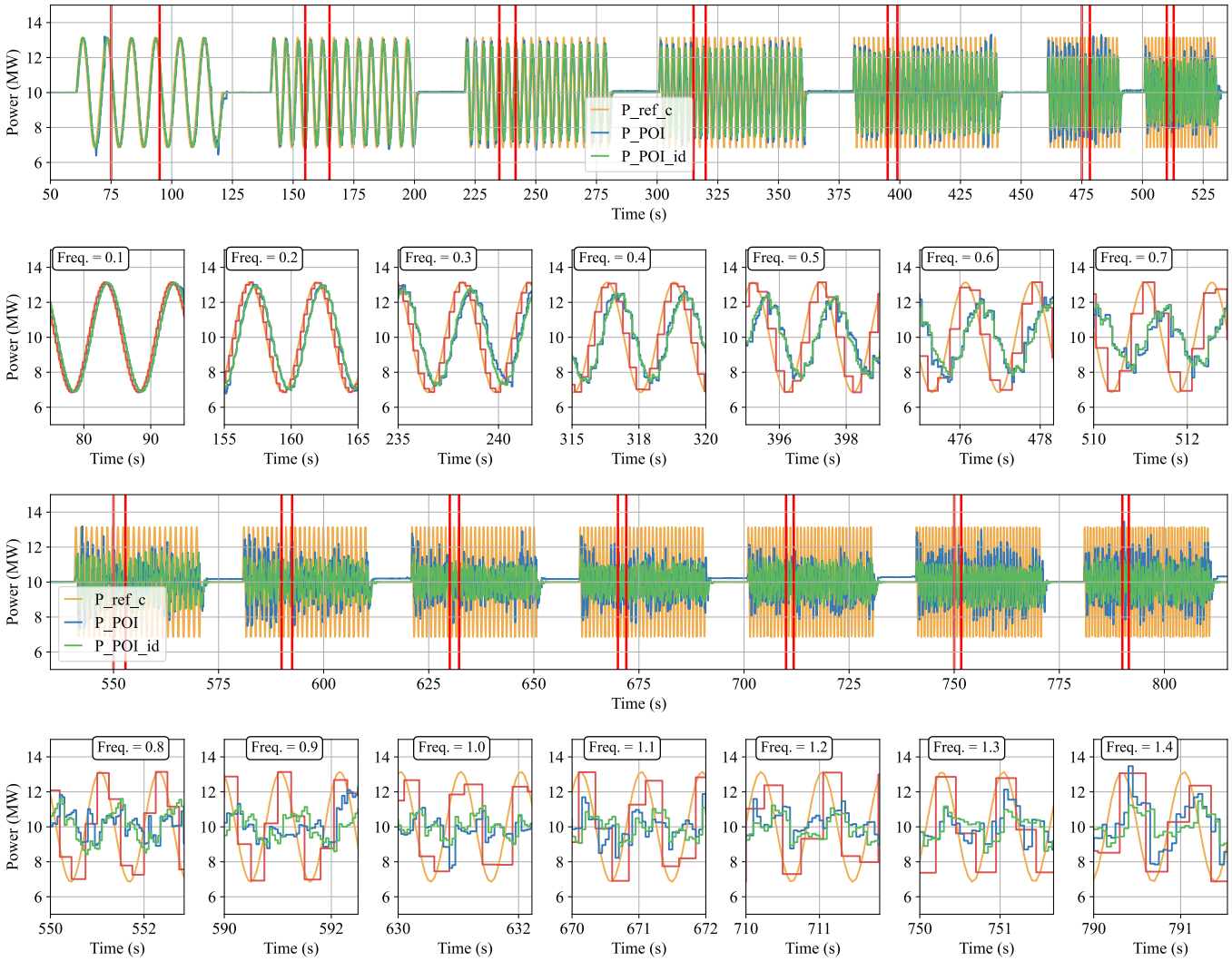

Fig. 3. SIMO Identification P_{POI}

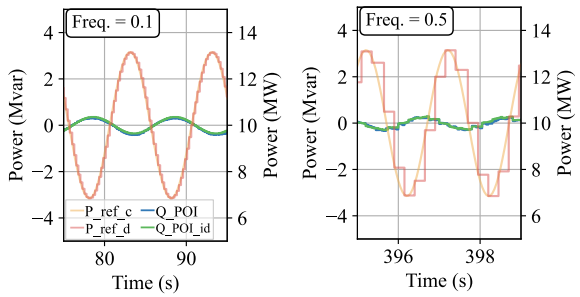

Fig. 4. SIMO Identification Q_{POI} for 0.1 and 0.5 Hz

$$A = \begin{bmatrix} 0.8741 & -0.0282 \\ 0.2574 & 0.7959 \end{bmatrix} \quad B = \begin{bmatrix} -0.0188 \\ -0.0095 \end{bmatrix}$$
$$C = \begin{bmatrix} -28.2278 & 0.1742 \end{bmatrix} \quad D = \begin{bmatrix} 0.0000 \end{bmatrix}$$

From the previous representation, the discrete TF depicted in (6) is obtained.

$$\frac{0.09707z - 0.06406}{z^2 - 1.67z + 0.703}\, dt = 0.05s \tag{6}$$

The continuous state-space representation of the identified system is derived from its discrete counterpart. The resulting continuous state-space formulation is expressed as follows:

$$A = \begin{bmatrix} -0.5183 & -0.1346 \\ 1.2298 & -0.8915 \end{bmatrix} \quad B = \begin{bmatrix} -0.0185 \\ 0.0437 \end{bmatrix}$$
$$C = \begin{bmatrix} -28.0935 & -3.1936 \end{bmatrix} \quad D = \begin{bmatrix} 0.0000 \end{bmatrix}$$

The continuous TF shown in (7) is derived from the previous representation:

$$\frac{0.3803s + 0.6288}{s^2 + 1.41s + 0.6276} \tag{7}$$

Both the discrete and continuous second-order TFs can be used for two key purposes: (1) to design and evaluate central controllers for the PV system, particularly in applications that require compensation for plant delay responses, and (2) to validate the performance of generic mathematical models of converters commonly employed in practice.

B. Validation

The identified SISO system is validated by comparing the Bode plot of the plant response (based on the P-SISO dataset from (2)) with the continuous transfer function (TF) from (7). Fourier analysis was applied within 0.1–1.0 Hz to extract the magnitude and phase of the measured data. In terms of magnitude, the model aligns well with the plant response at most frequencies, although the measured power shows slightly higher amplitudes at low frequencies. For the phase, while the phase shift of the real system exceeds that of the model at the highest frequencies, the model demonstrates excellent performance at the low frequencies of interest.

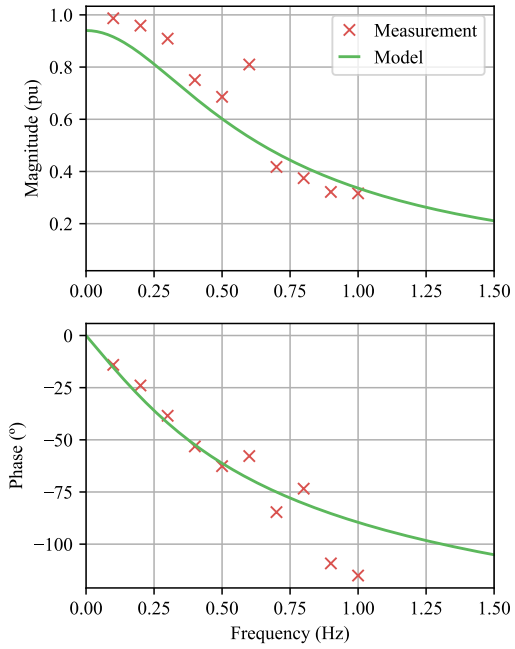

Fig. 5. Plant Bode. Real vs Identified SISO

V. Conclusions

This study presents a methodology for obtaining a model of a typical PV plant through simple and concise field tests that can be conducted during the commissioning phase. Using a widely used identification technique based on time-domain input-output measurements, two models are developed:

- A high-order SIMO model that captures the coupling between active and reactive power responses, demonstrating good performance across the frequency range, with accurate alignment in both magnitude and phase at the low frequencies relevant to inter-area oscillations.
- An equivalent low-order SISO model, provided in both discrete and continuous time domains, essential for the design and validation of centralised controllers. It shows satisfactory performance compared to the plant response, especially in its phase alignment at low frequencies.

Future work will focus on the design of a centralised POD controller to compensate for plant response delays while ensuring effective performance in the 0.1 to 1.5 Hz frequency range. Additionally, the identified model and the designed control will be integrated into a hardware-in-the-loop (HIL) environment in order to evaluate their performance in realistic operating conditions.

References

[1] ENTSO/E. *System Needs Study. System dynamic and operational challenges*, 05 2023. Available at https://tinyurl.com/392xvdu8.

[2] The European Commission. *Commission Regulation (EU) 2016/631 of 14 April 2016 establishing a Network Code on Requirements for Grid Connection of Generators*. Official Journal of the European Union, April 2016. Available at https://tinyurl.com/generatorseu.

[3] Naturgy CIDE REE, AELEC and ASEME. *Technical standard for monitoring the compliance of power generating modules according to EU Regulation 2016/631 version 2.1*, 7 2021. Available at https://tinyurl.com/4v5ybt3b.

[4] REE. *Guide for the implementation of power oscillation damping controllers. Version 2*, 09 2024. Available at https://tinyurl.com/bdz2r473.

[5] Federico Milano and Marian Anghel. Impact of time delays on power system stability. *IEEE Transactions on Circuits and Systems I: Regular Papers*, 59(4):889–900, 2012.

[6] EPRI. *Model User Guide for Generic Renewable Energy System Models. CA: 2023. 3002027129*, 10 2023.

[7] WECC. *Generic Solar Photovoltaic System Dynamic Simulation Model Specification*, 09 2012. Available at https://tinyurl.com/4azrxudf.

[8] FGW e.V. *Demands on Modelling and Validating Simulation Models of the Electrical characteristics of Power Generating Units and Systems, Storage Systems as well as for their Components. Revision 10*, 04 2022. Available at https://tinyurl.com/45eur32n.

[9] Welin Zhong, Muyang Liu, and Federico Milano. A co-simulation framework for power systems and communication networks. In *2019 IEEE Milan PowerTech*, pages 1–6, 2019.

[10] Kun Shi, Xuan Ren, Tao Da, Haixiang Sun, Dehu Zou, Fuming Cheng, and Wei Liu. Real-time co-simulation platform for cyber-physical power system based on 5g communication technology. In *2021 IEEE Sustainable Power and Energy Conference (iSPEC)*, pages 4052–4057, 2021.

[11] Peter Mihal, Martin Schvarcbacher, Bruno Rossi, and Tomáš Pitner. Smart grids co-simulations: Survey research directions. *Sustainable Computing: Informatics and Systems*, 35:100726, 2022.

[12] Njegos Jankovic, Javier Roldán-Pérez, Milan Prodanovic, and Luis Rouco. Centralised multimode power oscillation damping controller for photovoltaic plants with communication delay compensation. *IEEE Transactions on Energy Conversion*, 39(1):311–321, 2024.

[13] Daniel del Rivero, Pablo García, Cristian Blanco, and Ángel Navarro-Rodríguez. Control of aggregated virtual synchronous generators for pv plants considering communication delays. *IEEE Transactions on Industry Applications*, 60(4):6512–6523, 2024.

[14] MITECO. *Real Decreto 647/2020*, 7 2020. Available at https://www.boe.es/buscar/doc.php?id=BOE-A-2020-7439.

[15] MITECO. *Orden TED/749/2020, de 16 de julio, por la que se establecen los requisitos técnicos para la conexión a la red necesarios para la implementación de los códigos de red de conexión.*, 7 2020. Available at https://www.boe.es/eli/es/o/2020/07/16/ted749.

[16] Ning Zhou, J.W. Pierre, and J.F. Hauer. Initial results in power system identification from injected probing signals using a subspace method. *IEEE Transactions on Power Systems*, 21(3):1296–1302, 2006.

[17] Giuseppe Armenise Gabriele Pannocchia Riccardo Bacci di Capaci, Marco Vaccari. *Systems Identification Package for PYthon (SIPPY): User Guide*. University Of Pisa, Department of Civil And Industrial Engineering, Chemical Process Control Laboratory (CPCLAB), Pisa. Italy, May 2022. Available at https://github.com/CPCLAB-UNIPI/SIPPY.

[18] ENTSO-E. *Analysis of CE Inter-Area Oscillations of 1st December 2016*. ENTSO-E SG SPD Report, July 2017.